Peng, X.; Behl, M.; Zhang, P.; Mazurek-Budzyñska, M.; Feng, Y.; Lendlein, A.:

Synthesis of Well-Defined Dihydroxy Telechelics by (Co)polymerization of Morpholine-2,5-Diones Catalyzed by Sn(IV) Alkoxide.

In: Macromolecular Bioscience. Vol. 18 (2018) 12, 1800257.

First published online by Wiley: 14.10.2018

https://dx.doi.org/10.1002/mabi.201800257

Synthesis of well-defined dihydroxy telechelics by (co)polymerization of morpholine-2,5-diones catalyzed by Sn(IV) alkoxide

Xingzhou Peng, Marc Behl, Pengfei Zhang[#], Magdalena Mazurek-Budzyńska, Yakai Feng, Andreas Lendlein*

Dr. X. Peng, Dr. M. Behl, P. Zhang, Dr. M. Mazurek-Budzyńska, Prof. Y. Feng, Prof. A. Lendlein
Institute of Biomaterial Science and Berlin-Brandenburg Centre for Regenerative Therapies, Helmholtz-Zentrum Geesthacht, 14513 Teltow, Germany
Dr. X. Peng, P. Zhang, Prof. Y. Feng
School of Chemical Engineering and Technology, Tianjin University, Tianjin 300350, China Dr. X. Peng, Dr. M. Behl, P. Zhang, Prof. A. Lendlein
Institute of Chemistry, University of Potsdam, 14476 Potsdam, Germany
Dr. X. Peng, Dr. M. Behl, P. Zhang, Prof. Y. Feng, Prof. A. Lendlein
Tianjin University-Helmholtz-Zentrum Geesthacht Joint Laboratory for Biomaterials and Regenerative Medicine, 14513 Teltow, Germany

[#] Deceased

*Corresponding author. E-mail address: andreas.lendlein@hzg.de

Abstract: Well-defined dihydroxy telechelic oligodepsipeptides (oDPs), which have a high application potential as building blocks for scaffolds materials for tissue engineering applications or particulate carrier systems for drug delivery applications were synthesized by ring-opening polymerization (ROP) of morpholine-2,5-diones (MDs) catalyzed by 1,1,6,6-tetra-n-butyl-1,6-

distanna-2,5,7,10-tetraoxacyclodecane (Sn(IV) alkoxide). In contrast to ROP catalyzed by $Sn(Oct)_2$, the usage of Sn(IV) alkoxide leads to oDPs, with less side products and well-defined end-groups, which is crucial for potential pharmaceutical applications. A slightly faster reaction of the ROP catalyzed by Sn(IV) alkoxide compared to the ROP initiated by $Sn(Oct)_2$/EG was found. Copolymerization of different MDs resulted in amorphous copolymers with T_gs between 44 and 54 °C depending on the molar comonomer ratios in the range from 25 to 75%. Based on the well-defined telechelic character of the Sn(IV) alkoxide synthesized oDPs as determined by MALDI ToF measurements, they resemble interesting building blocks for subsequent postfunctionalization or multifunctional materials based on multiblock copolymer systems whereas the amorphous oDP-based copolymers are interesting building blocks for matrices of drug delivery systems.

1. Introduction

Oligodepsipeptides (oDPs), strictly alternating copolymers composed of α-amino acid and α-hydroxy acid repeating units, are known as an valuable addition to biomaterials apart from poly(α-amino acid)s and poly(α-hydroxy acid)s. Compared to poly(α-amino acid)s, whose degradation requires catalysis of an enzyme, oDPs can be degraded by hydrolysis because of the ester groups. On the other hand, compared to polyesters, oDPs provide higher Young's moduli caused by strong intermolecular hydrogen-bridge bonds formed between amide groups. Meanwhile, the physico-chemical properties can be tuned by variation of the amino acid moieties, for example, carboxylic acid groups can be introduced by incorporation of aspartic acid. Thus, telechelic oDPs show great promise as building blocks for biomedical applications.[1-7] Especially amorphous, solely depsipeptide-based, telechelics are interesting candidate materials for tissue engineering and drug delivery applications. [5, 8-15] Similar to telechelics based on polyesters, well-defined telechelic oDPs are the prerequisite when these oDPs should be used as functional building

blocks for follow-up reactions like multiblock copolymer synthesis by polyaddition reactions.[16, 17] In this way, the development of methods to achieve the well-defined oDPs is of high relevance. The classical synthesis route of oDPs is ring-opening polymerization (ROP) of morpholine-2,5-dione (MD) derivatives.[18, 19] Several nontoxic, organometallic and enzymatic catalysts as well as initiators have been examined for the synthesis of oDPs.[9] Tin(II) 2-ethylhexanoate ($Sn(Oct)_2$) is the most commonly used catalyst for the polymerization of MDs as well as their copolymerization with other cyclic monomers i.e. lactide and ε-caprolactone.[7, 20-22] However, ROP catalyzed by $Sn(Oct)_2$ still encounters the challenge of poor reaction control of the polymer molecular weight, as well as loss of terminal groups caused by the side reactions resulting from any hydroxyl-containing species and by transesterification reactions (typical inter- and intra- molecular reaction and backbiting transesterification and/or chain transfer reactions).[23] Impurities i.e. water and organic acids are diffluent in the polymerization in an undetected way by *in situ* formation of additional active species in the initiation phase of ROP.[24] Accordingly, in the copolymerization with other cyclic monomers the incorporated amounts of MDs among these copolymers were very low, typically between 5 and 10%.

In case of ROP catalyzed by $Sn(Oct)_2$, a tin alkoxide is formed from the $Sn(Oct)_2$ and the hydroxyl groups of initiator and acts as the active species during the ROP (Fig. S1). In this way an alternative choice as catalyst for the ROP of lactone based monomers is the usage of 1,1,6,6-tetra-*n*-butyl-1,6-distanna-2,5,7,10-tetraoxacyclodecane (Sn(IV) alkoxide), as demonstrated for the ROP of *L*-lactide, 1,5-dioxepan-2-one or ε-caprolactone.[25, 26]

In contrast to the application of $Sn(Oct)_2$, the synthesis of Sn(IV) alkoxide and subsequently its application in ROP can be considered as a promising approach to separate the induction and prolongation period of polymerization (Scheme 1). Meanwhile, Sn(IV) alkoxide is inherently

hydrophobic and can minimize the participation of moisture in the ROP. Furthermore, it is reported to catalyze transesterification reactions to a lower extent.[27] In this way, side reactions initiated by moisture should be kept to a minimum and high molecular weights should be obtainable. The termination of the Sn(IV) alkoxide polymerization is shown as Figure S2.

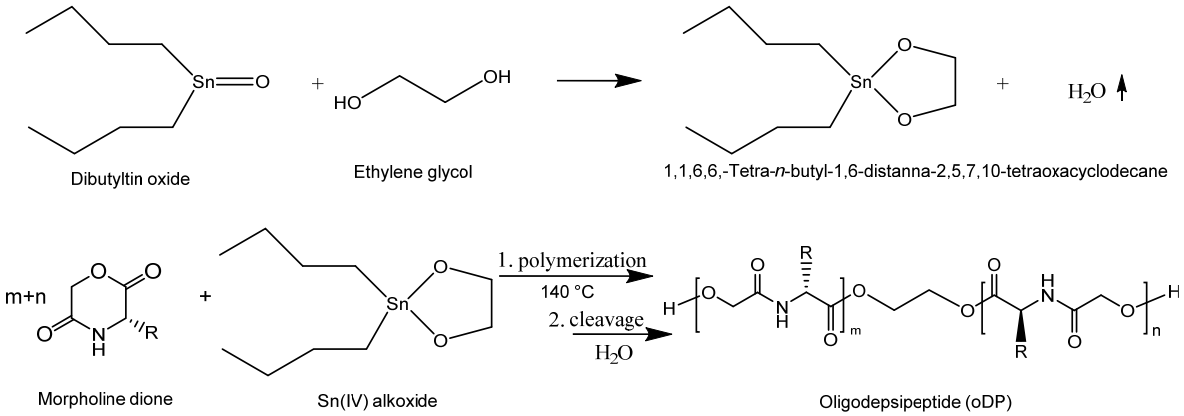

Mechanism:

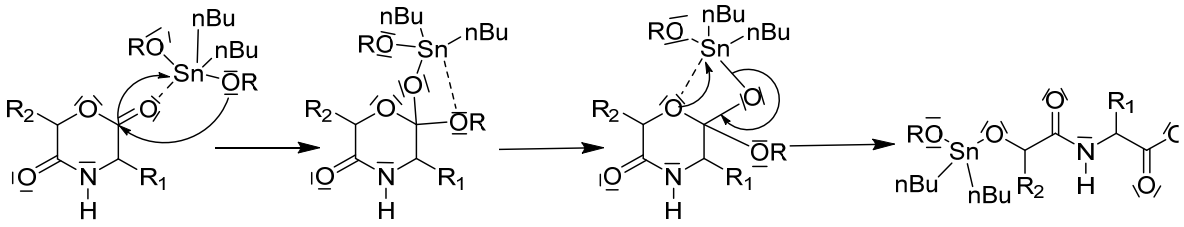

Scheme 1. Synthesis of 1,1,6,6-tetra-*n*-butyl-1,6-distanna-2,5,7,10-tetraoxacyclodecane (Sn(IV) alkoxide) and ring-opening polymerization of morpholine-2,5-diones.

We hypothesized that Sn(IV) alkoxide allows a more precise control of the ROP reaction and results in well-defined telechelic oDPs. The general applicability of the Sn(IV) alkoxide for the ROP of MDs was explored in a kinetic and thermodynamic study. Moreover, the Sn(IV) alkoxide

was utilized to investigate ROP copolymerization of different MDs to explore whether copolymer oDPs based solely on MD can be obtained. Based on ^{1}H and ^{13}C NMR analysis, as well as DSC measurements, the structure of random copolymers was confirmed and characterized.

2. Experimental

2.1. Materials

If not mentioned otherwise, catalyst and solvents were obtained from Sigma Aldrich (Seelze, Germany) and were used as received. Dibutyltin(IV) oxide (98%) was purchased from Th. Geyer (Hamburg, Germany), *L*-alanine, *L*-leucine and *L*-isoleucine were obtained from Roth (Karlsruhe, Germany). Tin(II) 2-ethylhexanoate ($Sn(Oct)_2$) was distilled three times before usage. Ethylene glycol (EG) (purity ≥ 99%) was dried by stirring over $MgSO_4$, then distilled under inert conditions, and finally stored above molecular sieves. Solvents were dried by standard methods and distilled prior to usage. Sn(IV) alkoxide was prepared from ethylene glycol (EG) and dibutyltin(IV) oxide as described in references.[28, 29] Formation of Sn(IV) alkoxide was confirmed by ^{1}H NMR analysis.

2.2. Methods

Nuclear Magnetic Resonance (NMR) spectra were recorded on a Bruker Avance spectrometer at room temperature (r.t.). In most cases, DMSO-d_6 was used as deuterated solvent, Sn(IV) alkoxide was dissolved in $CDCl_3$. The protonated species of the related solvent in deuterated solvent was used as an internal standard. Chemical shifts were referenced to DMSO-d_6 = 2.5 ppm and $CDCl_3$ = 7.3 ppm, respectively.

The thermal properties of the polymers were determined by differential scanning calorimetry (DSC) on a Netzsch DSC 204 (Selb, Germany), which was equipped with a low temperature cell. The cyclic measurements were conducted with a heating rate of 10 °C·min^{-1}. Samples were investigated

in the temperature range between -20 and 200 °C including the steps: heating from r.t. to 200 °C, then cooling to -20 °C, and finally heating again to 200 °C. After each step, samples were kept at the respective temperature for 2 min. The thermal transitions temperatures and enthalpies were determined from the second heating run.

Gel permeation chromatography (GPC) measurements were performed with a GPC system consisting of a GRAM gel column (250 × 4.6 mm^2, Polymer Standard Service, Mainz, Germany), a gradient pump PU 980, an automatic injector AS 851, a multi wavelength detector MD-910, a RI-930 detector (all Jasco, Tokyo, Japan), and a viscosimeter η-1001 detector (WGE, Dr. Bures, Dallgow, Germany). Dimethylformamide (DMF) was used as an eluent with a flow rate of 0.25 $mL \cdot min^{-1}$ at 35 °C. By determining the retention volumes from solutions of polystyrene standards in DMF, a universal calibration curve was obtained by plotting the $\log[\eta]_s M_s$ ($[\eta]_s$: intrinsic viscosity of the polystyrene in DMF, obtained from η-1001 detector; M_s: molar mass of the polystyrene standards) versus the retention volumes. The molecular weight of the polymer sample (M_u) was obtained according to the Mark-Houwink equation: $\log[\eta]_s M_s = \log[\eta]_u M_u$ ($[\eta]_u$: intrinsic viscosity of the polymer sample, obtained from η-1001 detector). Molecular weights (M_us) were calculated using the software Borwin-PDA Version 1.5 (Jasco, Tokyo, Japan) and WINGPC 6.2 (Polymer Standard Service, Mainz, Germany).

Matrix Assisted Laser Desorption/Ionization Time Of Flight Mass Spectroscopy (MALDI-TOF MS) was performed on a Biflex III spectrometer (Bruker Daltonik, Leipzig, Germany). Samples in amounts of 0.5 mg were dissolved in 1 mL tetrahydrofuran (THF). The solution of a mixture of *trans*-2-[3-(4-*tert*-butylphenyl)-2-methyl-2-propenylidene]malononitrile (DCTB) and potassium trifluoroacetate in THF was used as matrix.

Density measurements were carried out with an Ultrapycnometer 1000 instrument (Quantachrome, Odelzhausen, Germany) at r.t. The densities of 3-*sec*-butyl-morpholine-2,5-dione (BMD) and oligoBMD (oBMD) were 0.97 and 1.03 g·cm^{-3}, respectively.

2.3. Synthesis of monomers

Both monomers, 3-isobutyl-morpholine-2,5-dione (IBMD) and 3-*sec*-butyl-morpholine-2,5-dione (BMD), were synthesized in a modified two-step synthesis route according to the procedure described in reference.[22] In brief, in a first step the *N*-(hydroxyacetyl)amino acid was synthesized as an intermediate from the sodium salt of the amino acid and butyl glycolate, followed by the ring-closure reaction to the morpholine-2,5-dione (Scheme 2). The overall yields for IBMD and BMD were 25 and 31%, respectively.

Synthesis of (3*S*)-methylmorpholine-2,5-dione (MMD) was performed according to the synthesis procedure described in reference.[30] Detailed description of the synthesis can be found in the Supporting Information.

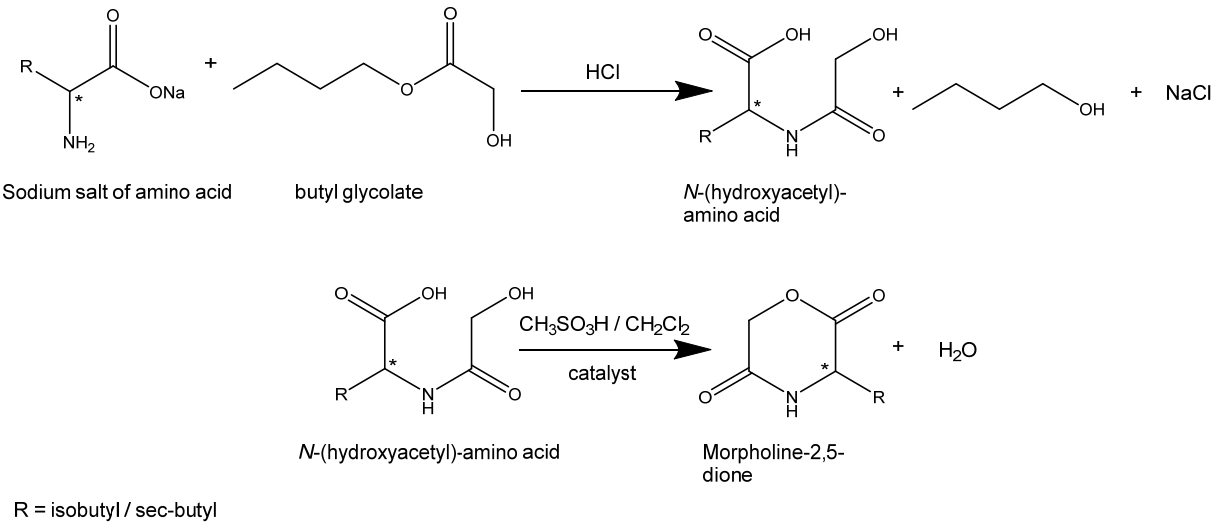

Scheme 2. Synthesis of morpholine-2,5-diones.

2.4. Synthesis of oDPs

A general procedure for the polymerization of MDs (10 mmol) based on using EG as initiator and either $Sn(Oct)_2$ or Sn(IV) alkoxide as catalyst. The degree of polymerization (DP) was set to 60 and the molar ratio of the catalyst and monomer was set to 1:100. The polymerizations were carried out in 10 mL pre-silanized Schlenk tubes equipped with magnetic stirrers. $Sn(Oct)_2$ was homogenously dispersed in dry toluene (1 M) and stored with 4 Å molecular sieve under inert gas. A mixture of the monomer and the required amount of initiator (as well as catalyst in case of $Sn(Oct)_2$) were weighed and placed into the reactor, protected by a stream of dry N_2. In case of solution polymerization, the adequate solvent (5 mL) was transferred by a water-free syringe to the reaction vessel, which was fitted with a condenser. In the next step, the reaction mixtures were heated to pre-defined temperatures (80 or 110 °C) and kept at this temperature for the required reaction time intervals. In case of bulk polymerization, the solvent used for transfer was removed by evaporation in vacuum (2 h). Afterwards, the reactor was refilled with inert gas and transferred to an oil bath at 230 °C to disperse the reactants under stirring for a few minutes. Then the reactor was immersed in a thermostated oil bath at 140 °C. When the polymerization reaction was completed, the reactor was cooled to r.t. The crude mixture was dissolved in 5 mL DMF and precipitated in a 20-fold amount of cold diethyl ether, and then dried in the oven at 45 °C until constant weight was achieved.

The kinetics of ROP were studied at 140 °C. Samples were taken at appropriate time intervals and the ROP was quenched by freezing in liquid nitrogen. The monomer conversions were determined by ^{1}H NMR via comparing the integrals of the monomer peak with the sum of integrals of the peaks from monomer and oligomers.

3. Results and discussion

3.1 Homopolymerization of BMD

The efficiency of Sn(IV) alkoxide initiator system in a ROP of MDs was explored in preliminary homopolymerization reactions of BMD owing to the good solubility of BMD in convenient solvents. The ROPs of BMD catalyzed by $Sn(Oct)_2$ with EG as co-initiator were performed for reference in parallel. Efficiencies of the reactions were evaluated by determining the monomer conversions after appropriate time intervals (Table 1). Sn(IV) alkoxide was successfully used for the ROP of *L*-lactide.[31] Reported results presented a fairly good control of reaction and relatively high monomer conversion (> 90%) when ROPs are carried out in homogeneous solutions at 60 °C. Because of the analogous structure of lactide and MD, a ROP in solution at moderate temperature was therefore chosen (Table 1, runs 1, 2, 4, and 5). Toluene appeared to be an ideal solvent for the reaction due to the good solubility of both catalysts and monomers at the reaction temperature as well as its reaction inertness. However, independently from the catalyst used, only a limited conversion of the monomer could be deduced from the ^{1}H NMR spectra of the obtained products. Furthermore, no precipitate was obtained after the purification, which is a hint that only low molecular weight compounds were obtained. These results can be attributed to: 1) a lower reaction activity of MD compared to *L*-lactide since a substituted amide group is inert towards ROP; 2) the thermodynamically disfavor of polymerizations carried out in solution.

When the polymerization was carried out as bulk polymerization at higher temperature (140 °C) as presented in Table 1, run 3 and 6, a tremendous increase of monomer conversion was observed. For the bulk polymerization catalyzed by $Sn(Oct)_2$, a monomer conversion of 82% with a yield of 62% was achieved. When the bulk ROP was initiated by Sn(IV) alkoxide, monomer conversion slightly increased to 89%, in addition to a higher yield of obtained precipitate (76%). The lower

yield of the reaction product of ROP catalyzed by $Sn(Oct)_2$ can be attributed to side reactions i.e. chain fragmentation in the later period of polymerization.[32] These fragmented polymer chains would have less repeating units and therefore are supposed to display a lower tendency for precipitation. Meanwhile, it is noteworthy to mention that $Sn(Oct)_2$ is capable to act as initiator. In this context, the theoretical DP is supposed to be lower than the ROP initiated by Sn(IV) alkoxide.

Table 1. ROP of BMD catalysed by $Sn(Oct)_2$ or Sn(IV) alkoxide.

Run	Catalyst /Initiator	Reaction condition	Time [h]	Conversion[a] [%]	Yield [%]
1	$Sn(Oct)_2$/EG	Toluene 80 °C	5	7	n.d.[c]
2	$Sn(Oct)_2$/EG	Toluene 110 °C	5	15	n.d.
3	$Sn(Oct)_2$/EG	Bulk 140 °C	5	82	62
4	Sn(IV) alkoxide	Toluene 80 °C	5	3	n.d.
5	Sn(IV) alkoxide	Toluene 110 °C	5	22	n.d.
6	Sn(IV) alkoxide	Bulk 140 °C	5	89	76
7[b]	$Sn(Oct)_2$/EG	Bulk 140 °C	24	91	65
8[b]	Sn(IV) alkoxide	Bulk 140 °C	24	88	79

[a] Estimated by ^{1}H NMR spectra measured in DMSO-d6.
[b] Polymerizations were performed for kinetic study, see Figure 1.
[c] n.d. : not determined

3.1.1. Kinetic study of ROP of BMD

In the kinetic study experiments of ROP, BMD was polymerized with $Sn(Oct)_2$/EG or Sn(IV) alkoxide (Table 1, run 7 and 8) at 140 °C. Samples were collected from the reaction mixture, dissolved in DMSO-d6, and analyzed by 500 MHz ^{1}H NMR. Typical NMR spectra are presented in Figure 1. The signal from the amide groups of monomer (δ = 8.58 ppm) was shifted to 8.35 ppm, which is characteristic for amide groups in oligomers. The monomer conversion was calculated using integrals of the signals from monomer and oligomer, respectively. After purification, the

final product was characterized by end group analysis by MALDI-TOF measurements.

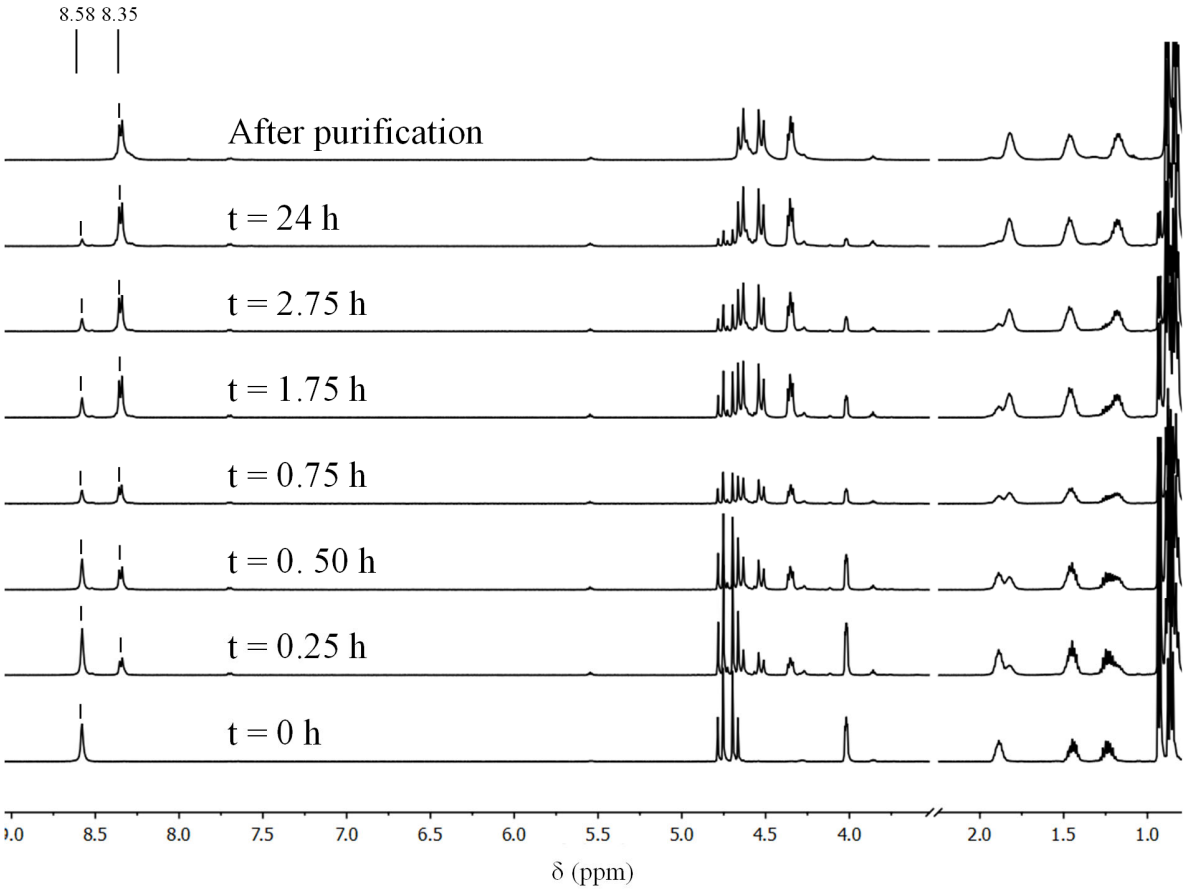

Figure 1: 500 MHz ^{1}H NMR spectra for the polymerization progress of BMD initiated by Sn(IV) alkoxide, see Supporting Information Figure S3 for signal assignment.

Figure 2 displays the time course of the monomer conversion in the ROP of BMD initiated by $Sn(Oct)_2$/EG or Sn(IV) alkoxide. In the starting period, the monomer conversion in reactions initiated by $Sn(Oct)_2$/EG was higher compared to reactions initiated by Sn(IV) alkoxide. This observation can be explained by the limited homogeneity of the dispersion of Sn(IV) alkoxide, in contrast to $Sn(Oct)_2$, providing a lower solubility.[28] Nonetheless, the two initiation systems did not differ significantly. The highest monomer conversion was achieved after 7.5 h for ROP initiated

by Sn(IV) alkoxide and remained almost constant when a thermodynamic equilibrium was achieved. In case of the ROP system catalyzed by $Sn(Oct)_2$, a slight increase of monomer conversion could be observed after a reaction time period of 7.5 h. This slightly higher monomer conversion can be attributed to side reactions i.e. chain fragmentation e.g. caused by 2-ethylhexanoate (Fig. S1), transesterification or degradation, as the thermodynamic equilibrium is catalyst or initiator independent. In addition, the coloration of the final product of ROP catalyzed by $Sn(Oct)_2$ also indicated the degradation reaction.

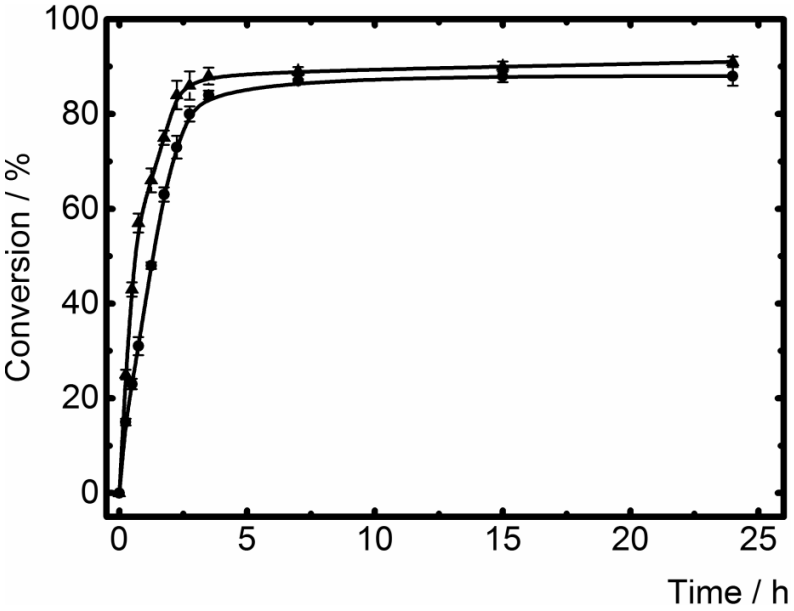

Figure 2: Homopolymerization of BMD initiated by $Sn(Oct)_2$/EG or Sn(IV) alkoxide; the dependence of monomer conversion on time. $Sn(Oct)_2$ /EG: triangle (▲); Sn(IV) alkoxide: circle (●).

The kinetic plots of the polymerization of the BMD are presented in semilogarithmic scale (Figure 3). After around 5 h, the ring-chain equilibrium or the thermodynamic equilibrium was achieved. Before that, a linear relationship between reaction time and monomer conversion can be observed. The time law for polymerization with ring-chain equilibrium can be expressed according

to equation (1):[33, 34]

$$ln\frac{M_0 - M_e}{M_t - M_e} = K_p[Cat][M]^* t = K_{app} t \quad (1)$$

M_0 is the monomer concentration in the starting mixture, M_e represents the monomer concentration at the moment when the reaction reaches the ring-chain equilibrium, M_t is the monomer concentration after a certain reaction time period, and M^* is the concentration of the particular active species.

The reactivity of initiator of the ROP system was quantified by the apparent rate constants K_{app}s (eq.1), which were determined from the slopes of the semilogarithmic-time curves. For $Sn(Oct)_2$/EG, K_{app} was 0.99 ± 0.03 h^{-1}, which is slightly higher than K_{app} for the ROP initiated by Sn(IV) alkoxide (0.89 ± 0.04 h^{-1}). The lower K_{app} in case of Sn(IV) alkoxide system can be explained by the inductive effect of the covalently bound alkyl groups of Sn(IV) atom, which further decrease the capability of the Sn(IV) atom to form the complex with the carbonyl oxygen of the ester group. In addition, the alkyl groups also sterically hinder the formation of the new tin-oxygen bonds.[35]

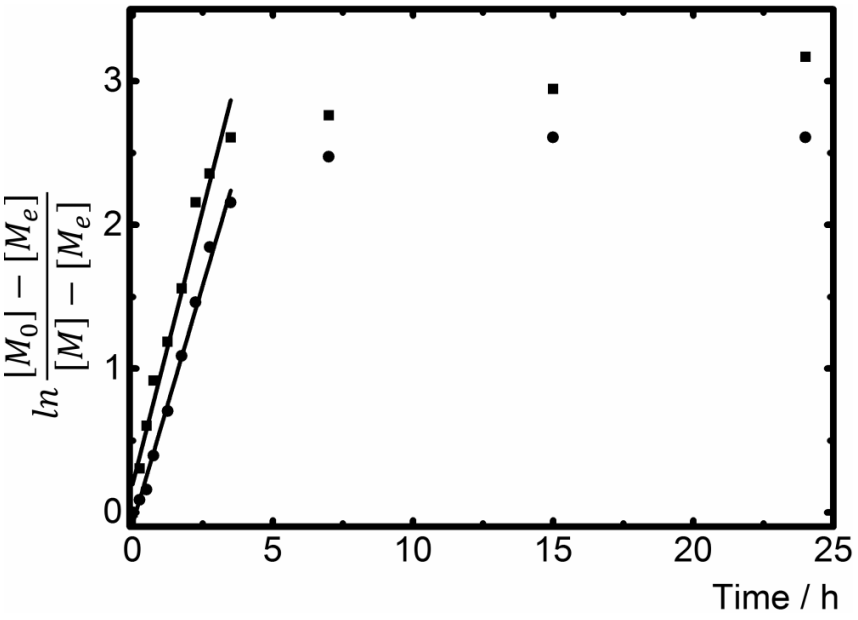

Figure 3: Homopolymerization of BMD in bulk initiated by $Sn(Oct)_2$/EG or Sn(IV) alkoxide: 1st order plot. $Sn(Oct)_2$/EG ; Sn(IV) alkoxide .

To evaluate the thermodynamic polymerization behavior of BMD, the standard enthalpy (ΔH_P^0) and entropy change (ΔS_P^0) during the polymerization can be determined based on Dainton´s equation (2).[34, 36]

$$\ln[M]_e = \frac{\Delta H_P^0}{RT} - \frac{\Delta S_P^0}{R} \quad (2)$$

Where T is the temperature (K), $[M]_e$ is the equilibrium monomer concentration and R is and the universal gas constant (8.31 $J \cdot K^{-1} \cdot mol^{-1}$).

From a practical point of view, the equilibrium monomer concentration $[M]_e$ can be substituted by the equilibrium molar fraction as demonstrated in equation (3):

$$[M]_e = \frac{[M]}{[M]_0} = \frac{n_m/V}{n_0/V} \quad (3)$$

Here, n_m represents the molar amount of monomer at equilibrium, n_0 the starting molar amount of the monomer, and V the volume of the polymerization mixture.

Figure 4a shows the influence of temperature (130 - 170 °C) on the monomer conversion in the ROP of BMD initiated by Sn(IV) alkoxide. An increase of the temperature resulted in a higher amount of monomer residues, which can be attributed to the left shift of the equilibrium towards exothermic polymerization upon an increase of temperature. According to the assumption that the volume of the bulk polymerization mixture was constant, Figure 4b shows a linear plot of the logarithm of $[M]_e$ as a function of the inverse of temperature. From the plot presented in Figure 4b, ΔH_P^0 = - 60.1 ± 0.6 $kJ \cdot mol^{-1}$ and ΔS_P^0 = - 127.8 ± 0.2 $J \cdot K^{-1} \cdot mol^{-1}$ were determined from the

slope and the y-intercept of the line, respectively. As expected, the monomer conversion decreased with the increase of reaction temperature.

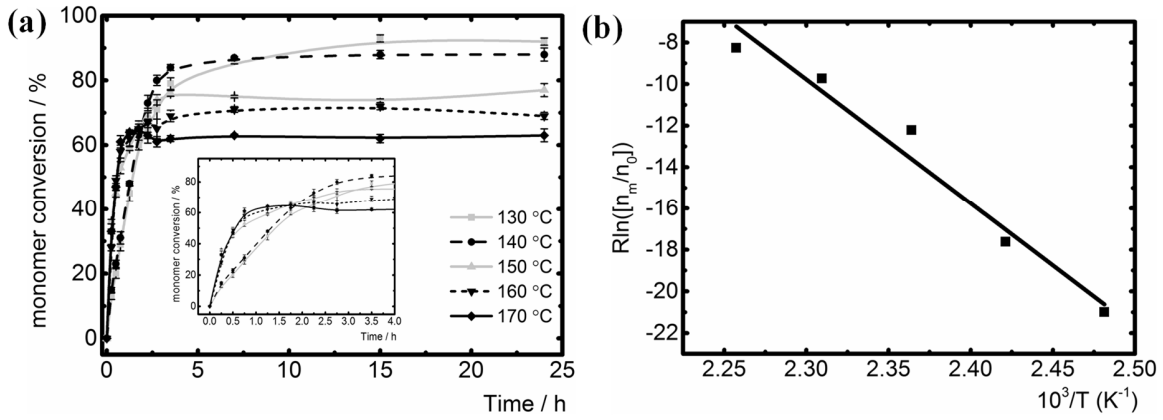

Figure 4: (a) The time course of the conversion of BMD for the ROP initiated by Sn(IV) alkoxide in the temperature range from 130 to 170 °C. (b) Dainton's plot of the ROP of BMD initiated by Sn(IV) alkoxide.

Compared with other cyclic monomers i.e. *D,L*-dilactide (ΔH_P^0 = - 96.1 ± 0.6 kJ mol^{-1} and ΔS_P^0 = - 39.6 ± 0.2 J K^{-1} mol^{-1}),[37] the thermodynamic results of ROP of BMD revealed a lower enthalpy and higher entropy in magnitude. In this case, the Gibbs free energy (ΔG_P) for the ROP of BMD has higher values than in case of ROP of *D,L*-dilactide, therefore it required more rigorous conditions. Again, the replacement of one ester bond of lactide with the amide bond in BMD can contribute to the more stable structure with lower tension in the monomer ring, and hence reduced the monomer activity.

MALDI-TOF MS of the obtained oligomers was performed to characterize the terminal groups (Figure 5). Five series of signals corresponding to four different species could be identified as shown in Figure 6a. Two series (3 and 4) correspond to telechelic oligomers doped by sodium and potassium as expected. Series 2 with a mass difference of 44 in relation to series 4 could originate

from water initiated polymerization. Potential explanation for this water initiated polymerization could be the hydrophilic nature of both $Sn(Oct)_2$ and EG despite of carful drying of reactants and inert condition during the polymerization reaction.

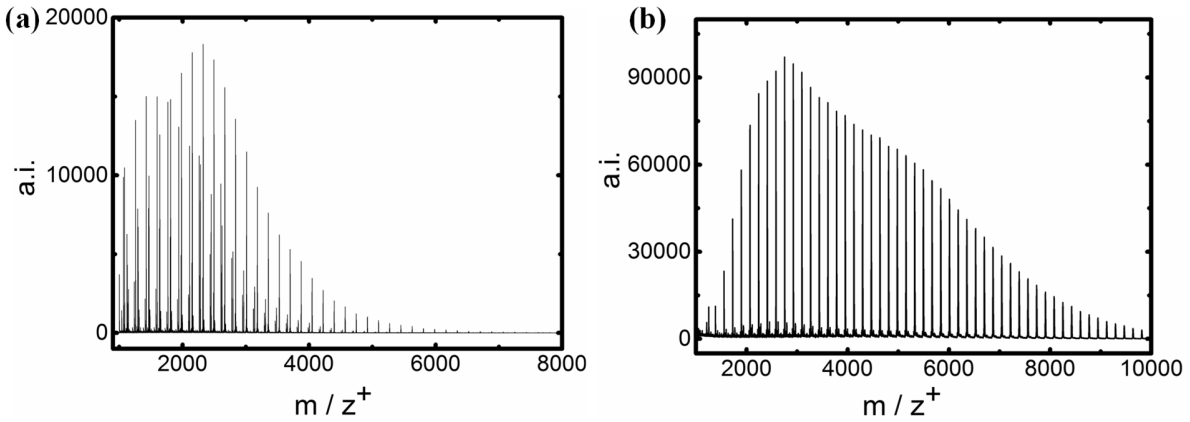

Figure 5: MALDI-TOF MS of oligomers based on BMD. Catalyst/initiator used: (a) $Sn(Oct)_2$/EG ; (b) Sn(IV) alkoxide.

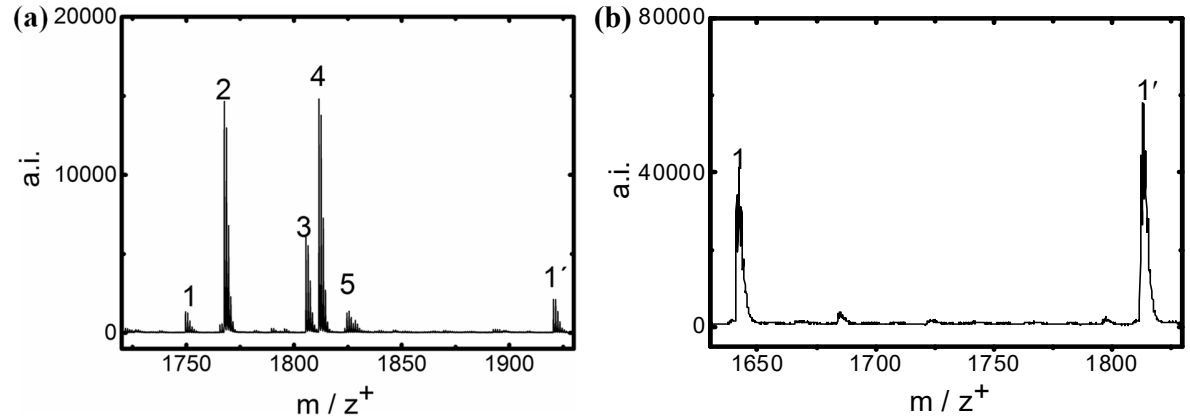

Figure 6: Detail spectra of MALDI-TOF MS of oligomers based on BMD. Catalyst/initiator used: (a) $Sn(Oct)_2$/EG and (b) Sn(IV) alkoxide.

Series 1 revealed the existence of macrocycles, which can be explained by intramolecular transesterification occurring in the progressed period of ROP, when side reactions become more

prominent. The molar mass of series 2 is 44 g·mol^{-1} less than the molar mass of series 4 and results from the polymer chains providing carboxylic terminal groups, which were initiated by traces of water or other active hydroxyl-containing species in the starting mixture. It is noteworthy to mention that except of these four predominant series an additional species could also be identified. We assumed that this additional species derives from the polymer chains terminated with methyl ester, which is resulting from a hydrolytic or alcoholytic cleavage. From these results it could be deduced that the ROP of BMD initiated by Sn(Oct)$_2$/EG will result in a weak control of reaction and in not well-defined telechelics.

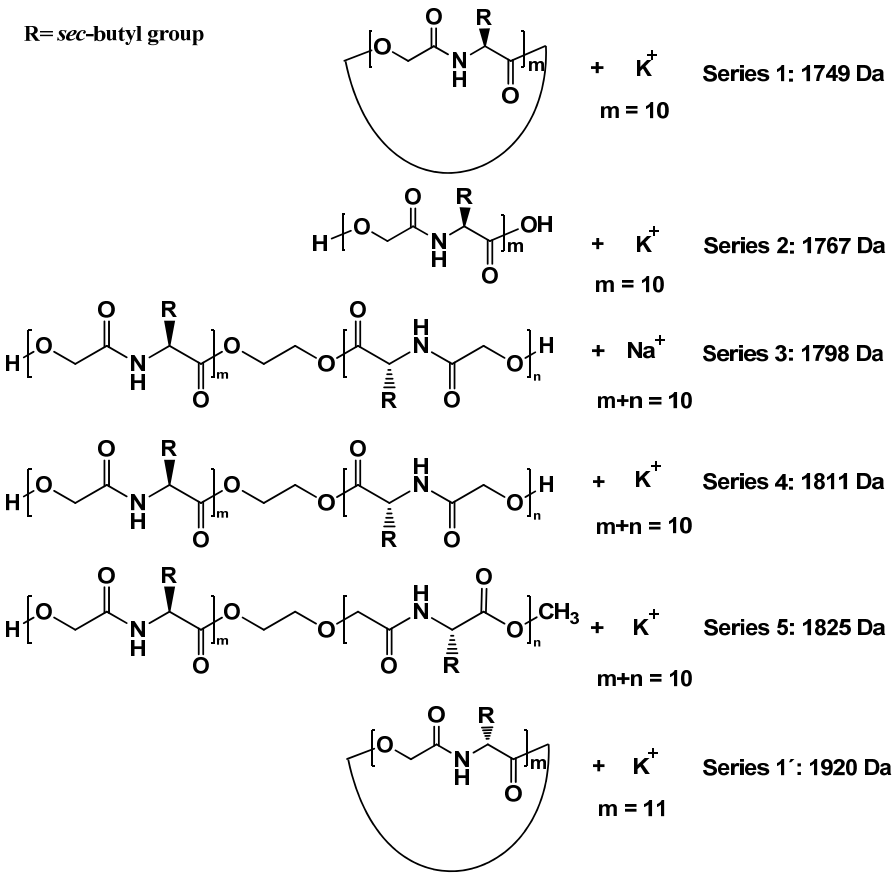

Figure 7. Structures of the species as assigned from mass spectrum of the oBMD synthesized with Sn(Oct)$_2$/EG.

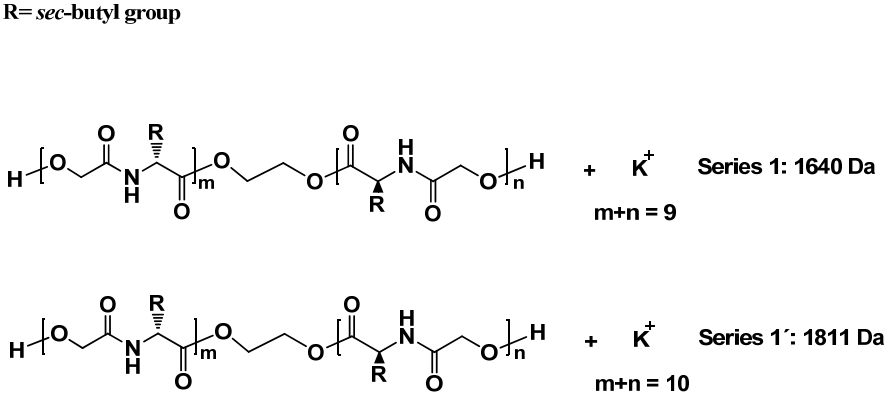

Figure 8. Structures of the species as assigned from mass spectrum of the oBMD synthesized with Sn(IV) alkoxide.

The structure of corresponding species identified based on the mass spectrum of the oBMD initiated by $Sn(Oct)_2$/EG are presented in Figure 7. In contrast, a lower number of signals can be observed in the MALDI-TOF spectrum of oBMD initiated by Sn(IV) alkoxide (Figure 6b). OH-terminated linear chains of series 1 and series 1´ were most abundant, which can be correlated to oligomers with 9 or 10 repeating units. The structure of the corresponding species identified from Figure 6b, are displayed in Figure 8. Surprisingly no macrocycles could be detected. These results revealed that: 1) the ROP of BMD is highly sensitive towards the hydrolytic cleavage; 2) Sn(IV) alkoxide can result in a better reaction control and more well-defined telechelic structures.

3.2. Copolymerization of MDs

Before the copolymerization behavior of the different MDs was explored, the kinetics of homopolymerizations of BMD, IBMD and MMD were investigated.

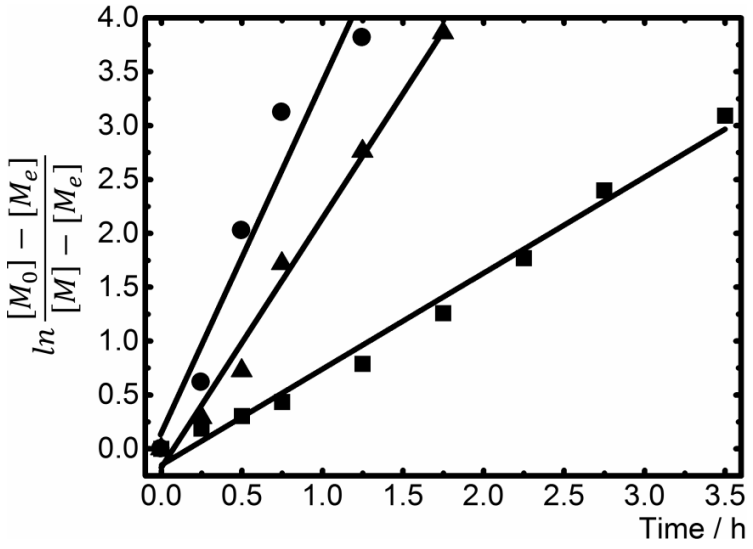

Figure 9. Homopolymerization of MDs in bulk initiated by Sn(IV) alkoxide: 1st order plot. BMD ■; IBMD ▲; MMD ●.

Figure 9 displays the ROP results of different MDs before the thermodynamic equilibria were reached. Similar to ROP of BMD plateaus of monomer conversion were reached for the polymerization of IBMD and MMD after 1.75 h and 1.25 h, which were 95% and 90%. Considering that the isopropyl group would have the highest +I effect but also the highest steric hindrance, the sec-butyl would have a lower +I effect and a similar steric hindrance compared to the isopropyl group, whereas the methyl group would have the lowest +I effect but also the lowest steric hindrance compared to the other groups, it can be speculated that the slightly higher conversion of the IBMD is governed more by the inductive effect rather than by the steric hindrance. Kinetic data revealed a K_{app} of MMD (3.25 h^{-1}) almost 4 times higher than that of BMD (0.89 h^{-1}). Interestingly, in case of BMD and IBMD, which possess side groups with the same sum of carbon atoms differing only in configuration, K_{app} of IBMD (2.31 h^{-1}) was 3 times higher than K_{app} of BMD. This difference in K_{app} can be explained by the different steric hindrance caused by difference in the configuration.

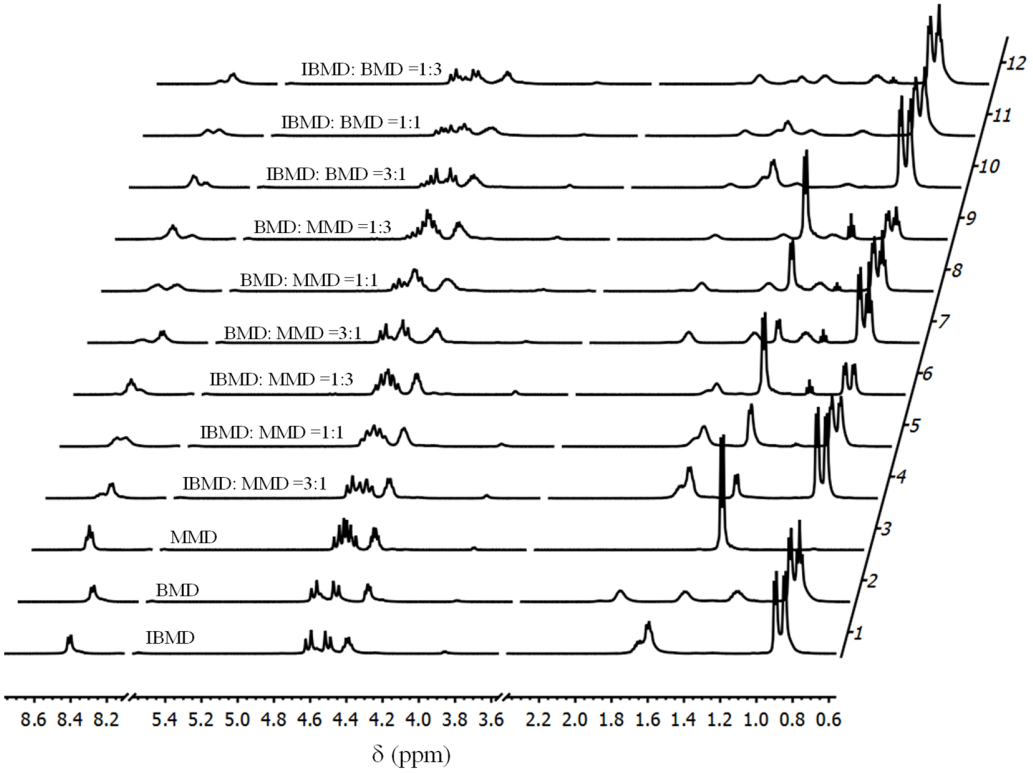

Figure 10. 500 MHz ^{1}H NMR spectra of the copolymers synthesized based on MMD, IBMD, and BMD catalyzed by Sn(IV) alkoxide, see Supporting Information Figure S4 for signal assignment.

Afterwards, copolymerization of MDs with various monomer ratios was performed. As seen in Figure 10, the spectra changed according to the comonomers and feed ratios. The enlarged spectrum in Figure 11a showed significant proton signals of the specific MDs. The doublets between 1.28 and 1.38 ppm were assigned to the methyl group in MMD units. The multiplets between 1.75 and 1.88 ppm, as well as 1.53 and 1.70 were assigned to the methylene and methine group in BMD and IBMD, respectively. The fraction of each monomer in the copolymer was quantified by the integral ratio of these groups of peaks. As listed in Table 2, different fractions in copolymers, which were determined by ^{1}H NMR, changed regularly with the variation of feed ratio. These results indicated that the composition of the copolymers correlated to the molar ratio of the monomers in the starting mixture.

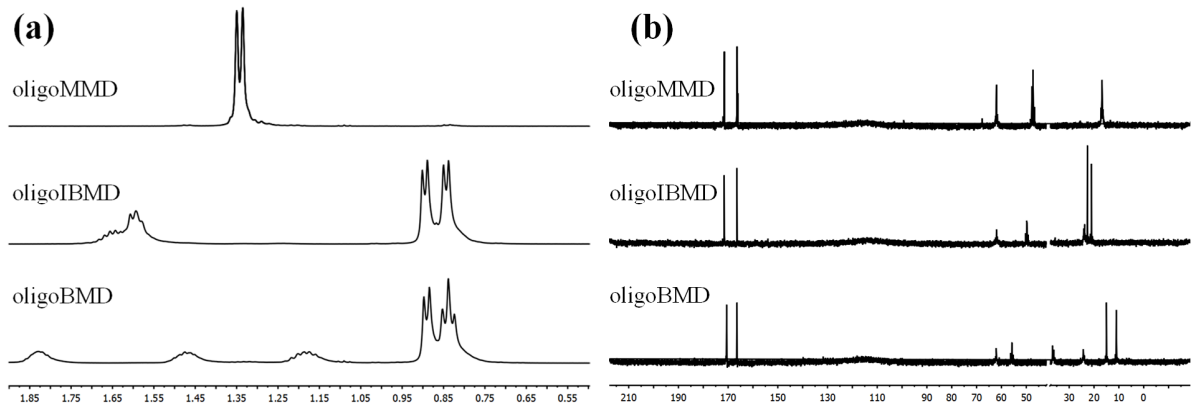

Figure 11. NMR spectra of homopolymers obtained from MMD, IBMD, and BMD catalyzed by Sn(IV) alkoxide. (a) 500 MHz ^{1}H NMR spectra; (b) 126 MHz ^{13}C NMR spectra.

Figure 11b displays the relevant signals in 126 MHz ^{13}C NMR spectra of different MDs. The triplets at 17 ppm were assigned to the methyl carbon in MMD units. Signal peaks at 10, 15 and 24 ppm were assigned to the methylene, methine and methyl group in BMD, respectively. Signal peaks at 21, 22, and 24 ppm were assigned to the methylene, methine and methyl group in IBMD, respectively. The molar ratio in copolymer is given by the ratio of integrals from these groups of peaks from 1024 scans. The composition in the polymer agrees well with initial composition of the feed mixture as deduced from ^{13}C and ^{1}H NMR (Table 2, 4th column)

Table 2. Characterization of all obtained homopolymers and copolymers: feed ratios, molecular weights, dispersity (D) and thermal properties

Run	Feed ratio (Mol Fraction)	Ratio[a] ^{1}H NMR	Ratio[b] ^{13}C NMR	$M_{n,NMR}$ kg·mol^{-1}	$M_{n,GPC}$ kg·mol^{-1}	D	T_g (°C)	T_m (°C)	$T_{g,theory}$[c] (°C)
1	IBMD : MMD = 1 : 1	1.0 : 1.1	1.0 : 1.0	6.8 ± 0.2	12 ± 0.1	1.6	54 ± 1	-	58
2	BMD : MMD = 1 : 1	1.0 : 1.0	1.0 : 1.0	6.8 ± 0.1	13 ± 0.1	1.6	48 ± 2	-	57
3	IBMD : BMD = 1 : 1	1.0 : 1.0	0.9 : 1.0	8.0 ± 0.1	12 ± 0.2	1.5	48 ± 1	-	51
4	IBMD			7.5 ± 0.2	11 ± 0.1	1.5	50 ± 2	180 ± 1	
5	BMD			10.1 ± 0.1	14 ± 0.2	1.5	52 ± 2	95 ± 3	
6	MMD			8.5 ± 0.2	13 ± 0.1	1.7	63 ± 1	136 ± 2	
7	IBMD : MMD = 3 : 1	2.8 : 1.0	2.9 : 1.0	7.1 ± 0.1	12 ± 0.3	1.5	54 ± 2	-	53
8	IBMD : MMD = 1 : 3	1.0 : 2.9	1.0 : 3.0	5.7 ± 0.2	11 ± 0.1	1.6	52 ± 2	-	59
9	BMD : MMD = 3 : 1	3.0 : 1.0	3.0 : 1.0	9.1 ± 0.1	16 ± 0.1	1.7	48 ± 2	-	54
10	BMD : MMD = 1 : 3	1.0 : 3.0	1.0 : 3.1	6.5 ± 0.2	12 ± 0.2	1.7	52 ± 1	-	60
11	IBMD : BMD = 3 : 1	2.9 : 1.0	2.9 : 1.0	7.6 ± 0.2	11 ± 0.1	1.8	49 ± 2	-	51
12	IBMD : BMD = 1 : 3	1.0 : 3.5	1.0 : 3.2	8.3 ± 0.1	11 ± 0.2	1.7	44 ± 1	-	52

[a] Molar ratio of each type of repeating units of the copolymer, measured by 500 MHz ^{1}H NMR spectra (16 scans).

[b] Molar ratio of each type of repeating units of the copolymer, measured by 126 MHz ^{13}C NMR spectra (1024 scans).

[c] theoretical value based on Flory-Fox equation

Various methods have been proposed to analyze the randomness and sequence length of the monomers units. In accordance to investigations reported in references,[38-40] ^{13}C NMR was selected as method of choice for randomness and sequence analysis, as CO signals are most sensitive to sequence differences, whereas carbon atoms in other positions normally do not provide sequence information. However, due to the high similarity of the carbonyl groups in the backbones, the potential difference between a random and a blocky sequence were not reflected by a shift of the signals in the ^{13}C NMR spectra.

Thermal characterizations of the resultant oligomers were performed by DSC. All copolymers (Table 2) showed a single T_g. In case of copolymers, in contrast to the homopolymers (Table 2, run 4, 5, and 6), no melting exotherm was observed, suggesting that all copolymers were in the glassy state. Moreover, the T_gs agreed well with the theoretical value calculated by Fox-Flory equation (Table 2, 10th column). Lack of melting transition in DSC thermograms suggests that the copolymerization of different MDs resulted in copolymers, whose crystallization is hindered either by a random / alternating sequence or by a blocky structure, which is capable to hinder crystallization as well.

4. Conclusion and Outlook

In summary, the results obtained in this work demonstrate that homo- or copolymerizations of different MDs can be efficiently initiated by Sn(IV) alkoxide. BMD was selected to be polymerized by both systems of $Sn(Oct)_2$/EG and Sn(IV) alkoxide for comparison. The kinetic data revealed that the apparent rate constant of ROP initiated by $Sn(Oct)_2$/EG system (0.99 ± 0.03 h^{-1}) was slightly higher than that of Sn(IV) alkoxide (0.89 ± 0.04 h^{-1}). In case of ROP of BMD initiated by Sn(IV) alkoxide, the thermodynamic parameters were also explored. ΔH_P^0 = - 60.1 ± 0.6 kJ mol^{-1} and ΔS_P^0 = - 127.8 ± 0.2 J K^{-1} mol^{-1} could be estimated based on

the assumption that the strain of the ring is independent of the concentration and solvent. End group analysis of oDPs was performed by means of MALDI-TOF, showing that the application of Sn(IV) alkoxide lead to a more precise control of the reaction and results in a well-defined structure in contrast to $Sn(Oct)_2$. Copolymerizations of different MDs initiated by Sn(IV) alkoxide were performed with various monomer ratios. The composition of the copolymers could be adjusted by controlling the feed ratios of monomer mixture. DSC results revealed glassy copolymers, either attributed to a hindered crystallization or to a potential random sequence structure of the monomer units. Based on the well-defined telechelic character of the oDPs, they resemble interesting building blocks for subsequent postfunctionalization or multifunctional materials based on multiblock copolymers like nanoparticulate gene carrier systems.[1, 15, 41] The amorphous cooligomers could also serve as solely depsipeptide-based degradable matrices in controlled drug release systems.[42] Their capability of exhibiting strong physical interactions might contribute to obtain higher drug loading or sustained release.[21] The copolymers providing T_gs few degrees above body temperature could also be used for solely depsipeptide based smart implants capable of a shape-memory effect, in which the depsipeptide segment would act as switching segment.[4, 22]

Supporting Information

Supporting Information is available from the Wiley Online Library or from the author.

Acknowledgments:

This work was financially supported by the Helmholtz-Association through programme-oriented funding, the Tianjin University-Helmholtz-Zentrum Geesthacht Joint Laboratory for Biomaterials and Regenerative Medicine, which is financed by the German Federal Ministry of Education and Research (BMBF, Grant No. 0315496), and the Chinese Ministry of Science and Technology (MOST, 2013DFG52040), as well as by the Deutsche Forschungsgemeinschaft

(DFG) through the Collaborative Research Centre 1112 “Nanocarriers”, subproject A03. X.P. gratefully acknowledges funding by the China Scholarship Council (CSC) (grant No. 201206250098).

Keywords: ring-opening polymerization, tin(II) 2-ethylhexanoate, Sn(IV) alkoxide, oligodepsipeptides, telechelics

References

[1] F. Yamamoto, R. Yamahara, A. Makino, K. Kurihara, H. Tsukada, E. Hara, I. Hara, S. Kizaka-Kondoh, Y. Ohkubo, E. Ozeki, S. Kimura, *Nucl. Med. Biol.* **2013**, *40*, 387.
[2] L. X. Zhao, N. N. Li, K. M. Wang, C. H. Shi, L. L. Zhang, Y. X. Luan, *Biomaterials* **2014**, *35*, 1284.
[3] R. Luxenhofer, C. Fetsch, A. Grossmann, *J. Polym. Sci., Part A: Polym. Chem.* **2013**, *51*, 2731.
[4] W. Yan, L. Fang, U. Noechel, K. Kratz, A. Lendlein, *Express Polym. Lett.* **2015**, *9*, 624.
[5] Y. K. Feng, W. Liu, X. K. Ren, W. Lu, M. Y. Guo, M. Behl, A. Lendlein, W. C. Zhang, *Polymers-Basel* **2016**, *8*, 58.
[6] L. C. Bai, Q. Li, X. H. Duo, X. F. Hao, W. C. Zhang, C. C. Shi, J. T. Guo, X. K. Ren, Y. K. Feng, *RSC Adv.* **2017**, *7*, 39452.
[7] L. Elomaa, Y. Q. Kang, J. V. Seppala, Y. Z. Yang, *J. Polym. Sci., Part A: Polym. Chem.* **2014**, *52*, 3307.
[8] G. Altankov, F. Grinnell, T. Groth, *J. Biomed. Mater. Res., Part A* **1996**, *30*, 385.
[9] Y. Feng, J. Lu, M. Behl, A. Lendlein, *Macromol. Biosci.* **2010**, *10*, 1008.
[10] Y. Ohya, T. Nakai, K. Nagahama, T. Ouchi, S. Tanaka, K. Kato, *J. Bioact. Compat. Polym.* **2006**, *21*, 557.
[11] Y. Ohya, H. Matsunami, E. Yamabe, T. Ouchi, *J. Biomed. Mater. Res., Part A* **2003**, *65*, 79.
[12] N. K. Abayasinghe, K. P. U. Perera, C. Thomas, A. Daly, S. Suresh, K. Burg, G. M. Harrison, D. W. Smith, *J. Biomater. Sci., Polym. Ed.* **2004**, *15*, 595.
[13] Y. Ohya, H. Matsunami, T. Ouchi, *J. Biomater. Sci., Polym. Ed.* **2004**, *15*, 111.
[14] A. C. Fonseca, M. H. Gil, P. N. Simões, *Prog. Polym. Sci.* **2014**, *39*, 1291.
[15] W. W. Wang, T. Naolou, N. Ma, Z. J. Deng, X. Xu, U. Mansfeld, C. Wischke, M. Gossen, A. T. Neffe, A. Lendlein, *Biomacromolecules* **2017**, *18*, 3819.
[16] A. Lendlein, P. Neuenschwander, U. W. Suter, *Macromol. Chem. Phys.* **2000**, *201*, 1067.
[17] A. L. Sisson, D. Ekinci, A. Lendlein, *Polymer* **2013**, *54*, 4333.
[18] C. Shi, F. Yao, Q. Li, M. Khan, X. Ren, Y. Feng, J. Huang, W. Zhang, *Biomaterials* **2014**, *35*, 7133.
[19] T. Naolou, A. Lendlein, A. T. Neffe, *Eur Polym J* **2016**, *85*, 139.
[20] P. J. A. in 't Veld, P. J. Dijkstra, J. H. van Lochem, J. Feijen, *Makromol. Chem.* **1990**, *191*, 1813.
[21] L. Zhang, Y. Feng, H. Tian, M. Zhao, M. Khan, J. Guo, *J. Polym. Sci., Part A: Polym. Chem.* **2013**, *51*, 3213.
[22] Y. Feng, M. Behl, S. Kelch, A. Lendlein, *Macromol. Biosci.* **2009**, *9*, 45.
[23] S. Penczek, A. Duda, A. Kowalski, J. Libiszowski, K. Majerska, T. Biela, *Macromol. Symp.* **2000**, *157*, 61.
[24] R. F. Storey, J. W. Sherman, *Macromolecules* **2002**, *35*, 1504.
[25] N. Andronova, A.-C. Albertsson, *Biomacromolecules* **2006**, *7*, 1489.
[26] J. M. Becker, R. J. Pounder, A. P. Dove, *Macromol. Rapid Commun.* **2010**, *31*, 1923.
[27] T. Redin, A. Finne‐Wistrand, T. Mathisen, A. C. Albertsson, *J. Polym. Sci., Part A: Polym. Chem.* **2007**, *45*, 5552.
[28] K. Stridsberg, A. C. Albertsson, *J. Polym. Sci., Part A: Polym. Chem.* **1999**, *37*, 3407.
[29] J. Bornstein, B. R. Laliberte, T. M. Andrews, J. C. Montermoso, *J. Org. Chem.* **1959**, *24*, 886.
[30] Y. Feng, C. Chen, L. Zhang, H. Tian, W. Yuan, *Trans. Tianjin Univ.* **2012**, *18*, 315.
[31] K. Stridsberg, A. C. Albertsson, *J. Polym. Sci., Part A: Polym. Chem.* **2000**, *38*, 1774.
[32] V. Jörres, H. Keul, H. Hoecker, *Macromol. Chem. Phys.* **1998**, *199*, 835.
[33] P. Rempp, E. Merrill, " *Polymer Synthesis*", Hüthig & Wepf, Basel, Heidelberg, New York, 1991.
[34] P. Dubois, O. Coulembier, J.-M. Raquez, "*Handbook of Ring-opening Polymerization*", John Wiley & Sons, 2009.

[35] R. F. Storey, B. D. Mullen, G. S. Desai, J. W. Sherman, C. N. Tang, *J. Polym. Sci., Part A: Polym. Chem.* **2002**, *40*, 3434.
[36] F. S. Dainton, K. J. Ivin, *Q. Rev., Chem. Soc.* **1958**, *12*, 61.
[37] B. C. Norris, D. G. Sheppard, G. Henkelman, C. W. Bielawski, *J. Org. Chem.* **2010**, *76*, 301.
[38] N. Nomura, A. Akita, R. Ishii, M. Mizuno, *J. Am. Chem. Soc.* **2010**, *132*, 1750.
[39] H. R. Kricheldorf, I. Kreiser, *Makromol. Chem.* **1987**, *188*, 1861.
[40] H. R. Kricheldorf, T. Mang, J. M. Jonté, *Macromolecules* **1984**, *17*, 2173.
[41] Q. Li, C. Shi, W. Zhang, M. Behl, A. Lendlein, Y. Feng, *Advanced Healthcare Materials* **2015**, *4*, 1225.
[42] T. Ouchi, M. Sasakawa, H. Arimura, M. Toyohara, Y. Ohya, *Polymer* **2004**, *45*, 1583.